Segmentation of Medical Images with Regional Inhomogeneities

D.K. Iakovidis✦, M.A. Savelonas✦, S.A. Karkanis✧, D.E. Maroulis✦
✦*Dept. of Informatics and Telecommunications, University of Athens, Greece*
✧*Dept. of Informatics and Comp. Tech., Lamia Institute of Technology, Greece*
rtsimage@di.uoa.gr

Abstract

This paper presents a novel deformable model for accurate delineation of regions of interest in medical images that contain regional inhomogeneities. Such images are common in various medical imaging domains including endoscopy and radiology. The proposed model improves the Active Contour Without Edges (ACWE) model by excluding sparse regional inhomogeneities from both the foreground and the background of the images to be segmented. The proposed model is tolerant to noise and allows for the delineation of multiple objects. Experiments were performed on both endoscopic and ultrasonic images from different organs. The results show that the proposed model can be effectively utilized for the delineation of abnormal tissue findings, and in presence of regional inhomogeneities it can be more accurate compared with the ACWE model.

1. Introduction

Medical image segmentation has been the focus of image analysis and pattern recognition research since the early beginnings of the seventies [1]. Since then a variety of relevant computational approaches have been proposed, many of which have been reviewed in [3]-[6]. Recent approaches that have been efficiently utilized for the recovery of shapes of the human body include the level set deformable models [5]-[6].

Deformable models are capable of recovering the shape of objects in images by following a contour deformation process. The deformation is realized by the minimization of an energy functional designed so that its local minimum is reached at the target boundaries. The energy functional in its basic form comprises a term that controls the smoothness of the contour and an image dependent term that forces the contour towards the boundaries of the objects. The level set approach to deformable models is more flexible compared to other approaches because it allows for topological changes of the contour during its evolution and is therefore capable of detecting multiple objects in an image.

State of the art level set deformable models include the Active Contour Without Edges (ACWE) model [7]. In this model the deformation of the contour is derived from the minimization of a reduced form of the Mumford-Shah energy functional [8], where the segmented image is restricted to two piecewise constant regions outside and inside the contour. The ACWE model does not utilize any edge related information, thus leading to noise tolerant image segmentation. Recent medical imaging applications of ACWE have demonstrated its advantageous performance over other relevant methods [9]-[10].

However, the assumption of piecewise constant regions outside and inside the contour is violated in the presence of regional inhomogeneities, which usually appear as single or multiple intensity spikes. Such inhomogeneities may be attributed either to the characteristics of the tissue being examined, or to external causes usually related to the imaging devices used.

Surpassing the aforementioned limitation of the ACWE model could possibly result in the enhancement of its segmentation performance in medical images with regional inhomogeneities. To reach this aim, we introduce a novel, improved deformable model that assumes piecewise constancy over regions outside and inside the contour that excludes sparse regional inhomogeneities. Its performance is evaluated for the delineation of abnormal tissue findings in various endoscopic and ultrasonic medical images with regional inhomogeneities, from different organs.

The rest of this paper comprises three sections. Section 2 describes the proposed model in contrast to the ACWE model. Experimental results are presented in Section 3, and finally Section 4 summarizes the conclusions of this study.

0-7695-2521-0/06/$20.00 (c) 2006 IEEE

2. Level Set Deformable Models

2.1. The Active Contour Without Edges model

The ACWE model as posed in [11] has the form of a minimization problem: Let Ω be a bounded open subset of R^2 and $\partial\Omega$ its boundary. We seek for the infimum of the energy functional $F(c^+, c^-, C)$,

$$\begin{aligned} F(c^+, c^-, C) &= \mu \cdot Length(C) \\ &+ \lambda_1 \int_{inside(C)} |u_0(x,y) - c^+|^2 \, dxdy \\ &+ \lambda_2 \int_{outside(C)} |u_0(x,y) - c^-|^2 \, dxdy \end{aligned} \quad (1)$$

where $u_0 : \Omega \to R$ is the input image, $C(s) : [0,1] \to R^2$ is a piecewise parameterized curve, c^+ and c^- represent the average value of u_0 inside and outside the curve and parameters $\mu > 0$ and $\lambda_1, \lambda_2 > 0$ are weights for the regularizing term and the fitting terms, respectively.

In the level set method, $C \subset \Omega$ is represented by the zero level set of a function $\phi : \Omega \to R$, such that

$$\begin{aligned} &C = \{(x,y) \in \Omega : \phi(x,y) = 0\}, \\ &inside(C) = \{(x,y) \in \Omega : \phi(x,y) > 0\}, \\ &outside(C) = \{(x,y) \in \Omega : \phi(x,y) < 0\} \end{aligned} \quad (2)$$

The average foreground (inside the contour) and background (outside the contour) intensities c_1 and c_2 are determined by

$$c_1(\phi) = \frac{\int_\Omega u_0(x,y) H(\phi(x,y)) dxdy}{\int_\Omega H(\phi(x,y)) dxdy} \quad (3)$$

$$c_2(\phi) = \frac{\int_\Omega u_0(x,y)(1 - H(\phi(x,y))) dxdy}{\int_\Omega (1 - H(\phi(x,y))) dxdy} \quad (4)$$

where H is the Heaviside function. By keeping c_1 and c_2 fixed, and minimizing F with respect to ϕ, the associated Euler-Langrange equation for ϕ is deduced. Finally, ϕ is determined by parameterizing the descent direction by an artificial time $t \geq 0$, and by solving the following equation

$$\frac{\partial \phi}{\partial t} = \delta(\phi)[\mu \cdot div(\frac{\nabla \phi}{|\nabla \phi|}) - \lambda^+ (u_0 - c_1)^2 + \lambda^- (u_0 - c_2)^2] = 0 \quad (5)$$

where δ is the one-dimensional Dirac measure and $t \in (0, \infty), (x,y) \in \Omega$.

2.2. The proposed deformable model

The proposed model considers sparse foreground and background regions which exclude the regional inhomogeneities. This is achieved by properly transcribing Eqs. (3)-(4).

We introduce two difference terms in the foreground and the background average intensities, defined by the following equation:

$$\Delta_i(x,y) = H(\phi(x,y) + a_i) - H(\phi(x,y)), \; i = 1, 2 \quad (6)$$

where $\alpha_1 \leq 0$ and $\alpha_2 \geq 0$ are application dependent constants, determined so that $[0, a_1]$ and $[-a_2, 0]$ define the acceptable ranges of $\phi(x,y)$ for a point (x,y) to be included in the sparse foreground and background region, respectively. Equation (6) implies that the points (x,y) for which $\phi(x,y)$ does not belong in the acceptable range result in $\Delta_i(x,y) \approx 0$. These points correspond to intensity inhomogeneities and cause abrupt changes of ϕ, resulting in $H(\phi(x,y) + a_i) = H(\phi(x,y))$.

Moreover, we assume that the initial contour as traced by ϕ_0, corresponds to a user defined region of interest and we employ $H(\phi_0)$ to restrict the calculation of the average foreground and background intensities c_1 and c_2 over this region. The Eqs. (3) and (4) are transcribed as follows

$$c_1(\phi) = \frac{\int_\Omega u_0(x,y) H(\phi(x,y)) H(\phi_0(x,y)) \Delta_1(x,y) dxdy}{\int_\Omega H(\phi(x,y)) H(\phi_0(x,y)) \Delta_1(x,y) dxdy} \quad (7)$$

$$c_2(\phi) = \frac{\int_\Omega u_0(x,y)(1 - H(\phi(x,y))) H(\phi_0(x,y)) \Delta_2(x,y) dxdy}{\int_\Omega (1 - H(\phi(x,y))) H(\phi_0(x,y)) \Delta_2(x,y) dxdy} \quad (8)$$

According to these, a point $(x,y) \in \Omega$ will not be included in the calculation of c_1 and c_2 if $\Delta_i(x,y) = 0$.

3. Results

A number of experiments were performed aiming to the assessment of the proposed model for the segmentation of medical images with regional inhomogeneities, in comparison with the original ACWE model. The delineation of abnormal tissue findings was identified as a common application context to focus the experiments on. The delineation of abnormal tissue masses for accurate recovery of their shape is important in medical diagnostics and in many

cases it is regarded as a malignancy risk factor [12]-[13].

A diverse dataset comprising of 38 medical images with regional inhomogeneities was utilized, including endoscopic images of gastric ulcers and ultrasound images of parotid tumors and thyroid nodules (Table 1). The images were digitized at 256×256-pixel dimensions and 8-bit grey level depth. Both α_1 and α_2 were empirically determined for the different kinds of images.

The quantification of the segmentation results was realized by measuring the overlap v between the region specified by the active contour models and the ground truth image region G was specified by three experts

$$v = \frac{A \cap G}{A \cup G} \tag{9}$$

Table 1. Datasets used in the experiments per subject and segmentation accuracy using ACWE and the proposed model, with respect to ground truth segmentations.

Subject	Images	ACWE v (%)	Proposed v (%)
Gastric Ulcers	12	91.7±1.2	93.4±0.9
Parotid Tumors	6	83.8±2.6	91.0±2.4
Thyroid Nodules	20	85.9±2.1	91.6±1.4

The segmentation results obtained with the ACWE and with the proposed improved model are summarized in Table 1. Figure 1 illustrates two indicative images used in the experiments. The first image (Fig. 1a) illustrates an endoscopic image of a benign gastric ulcer, with regional inhomogeneities attributed to the tissue's relief and the reflected light from the endoscope's illumination source (Fig. 1c). The overlap obtained with ACWE and with the proposed model is 96.4% (μ=650, λ_1=1 and λ_2=1, Fig. 1e) and 98.1% (μ=650, λ_1=1, λ_2=1, α_1=-10^{-12} and α_2=10^{-12}, Fig. 1g), respectively.

The second image (Fig. 1b) illustrates an ultrasound image of a parotid gland adenoma. The regional inhomogeneities in the ultrasound images are related to speckle, noise and the echogenicity of the examined tissue (Fig. 1d). The overlap obtained with the ACWE is 88.4% (μ=650, λ_1=5 and λ_2=5, Fig. 1f) whereas the overlap achieved with the proposed model is much higher reaching 94.2% (μ=650, λ_1=5, λ_2=5, α_1 =-10^{-13} and α_2=10^{-13}, Fig. 1h). It is worth noting that the difference in the overlap obtained with the ACWE and the proposed model in the second image is larger than in the first image. This can be explained, as the inhomogeneity inside and outside the abnormal tissue in the second image is larger. The local variance (σ^2), as a measure of inhomogeneity [14], inside and outside of the abnormal tissue but within the region of interest, in the second image is by 27.9% and 20.7% larger than in the first image respectively.

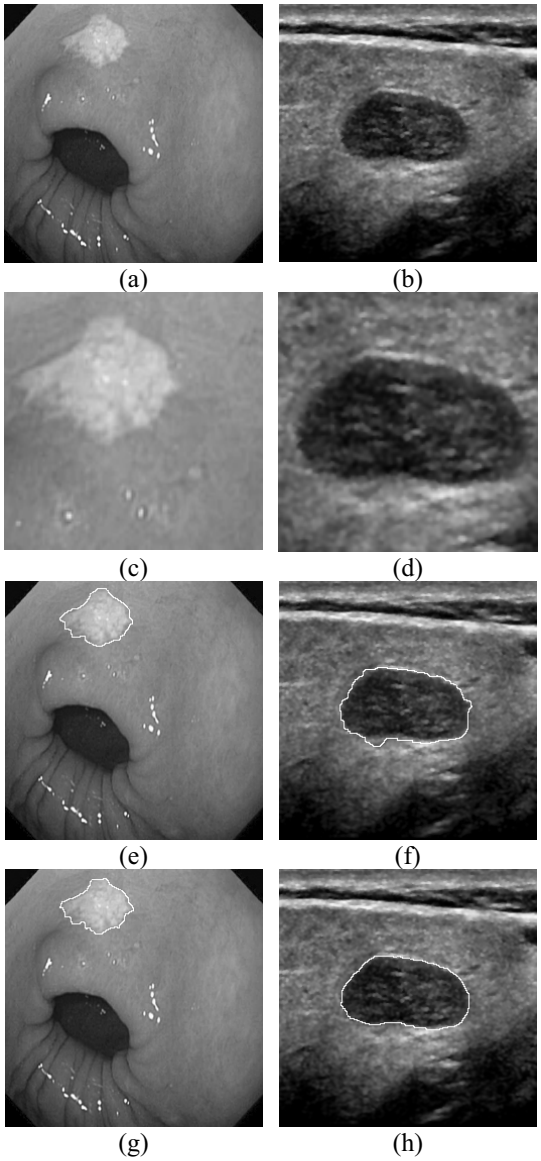

Figure 1. Medical images with regional inhomogeneities and segmentation results (a) endoscopic image of a benign gastric ulcer, (b) ultrasonic image of a parotid gland adenoma, (c-d) scaled images revealing the regional inhomogeneities inside and outside the abnormal tissue masses, (e-f) segmentation using ACWE model, (g-h) segmentation using the proposed model.

Similar observations are valid with respect to the average overlaps obtained between the endoscopic and ultrasound image classes.

The overlap differences observed in favor of the proposed model was significant (p<0.05) as validated by ANOVA (ANalysis Of VAriance), a statistical test for the heterogeneity of means by analysis of group variances [14].

4. Conclusions

We have introduced a novel, improved deformable model based on the ACWE model. The new model assumes piecewise constancy over sparse regions outside and inside the active contour. We applied it for the segmentation of medical images with regional inhomogeneities. The results show that in such images the proposed model outperforms ACWE in the delineation of abnormal tissue masses. The enhancement of the segmentation quality has been reported higher in images with more prevalent inhomogeneities inside and outside the abnormal tissue.

Future work includes a systematic evaluation of the proposed model on larger datasets of medical images acquired on regular basis, investigation of automatic parameter tuning approaches and the integration of the proposed model in a medical decision support system.

Acknowledgments

We would like to thank EUROMEDICA S.A. Greece for the provision of part of the medical images. We would also like to express our gratitude to Dr. N. Dimitropoulos, M.D., Radiologist, and Prof. M. Tzivras, M.D., Gastroenterologist for sharing their expertise in the interpretation of the medical images. This research was funded by the Operational Program for Education and Vocational Training (EPEAEK II) under the framework of the project “Pythagoras - Support of University Research Groups” co-funded by 75% from the European Social Fund and by 25% from national funds.

References

[1] J. Sklansky, and D. Ballard, “Tumor Detection in Radiographs,” Computer and Biomedical Research, vol. 6, no. 4, pp. 299-321, Aug. 1973.

[2] N. Kalouptsidis, Signal Processing Systems: Theory and Design, J. Wiley & Sons, NY, 1997.

[3] J.S. Duncan, and N. Ayache N., “Medical Image Analysis: Progress Over Two Decades and The Challenges Ahead,” IEEE Trans. Pattern Analysis Machine Intelligence, vol. 22, pp. 85-106, 2000.

[4] D. L. Pham, C. Xu, and J. L. Prince, "Current Methods in Medical Image Segmentation," Annual Review of Biomedical Engineering, vol. 2, pp. 315-338, 2000.

[5] J.S. Suri et al, “Shape Recovery Algorithms Using Level Sets in 2-D/3-D Medical Imagery: A State-of-the-Art Review”, IEEE Trans. on Inf. Tec. in Biomedicine, vol. 6, no. 1, pp. 8-28, Mar. 2002.

[6] T. McInerney, and D. Terzopoulos, “Deformable Models in Medical Image Analysis: A Survey,” Med Image Analysis 1996;1:91-108.

[7] T.F. Chan, L.A. Vesse, “Active Contours Without Edges”, IEEE Trans. Image Processing, vol. 7, pp. 266-277, Feb. 2001.

[8] D. Mumford, J. Shah, “Optimal Approximation by Piecewise Smooth Functions and Associated Variational Problems”, Commun.Pure Appl. Math., vol.42, pp 577-685, 1989.

[9] E.D. Angelini, T. Song, B.D. Mensh, A.F. Laine, Segmentation and quantitative evaluation of brain MRI data with a multi-phase three-dimensional implicit deformable model, SPIE International Symposium, Medical Imaging 2004, San Diego, CA USA, Vol. 5370, pp. 526-537, 2004, 2004.

[10] N. Lin, W. Yu, J.S. Duncan, “Combinative Multi-scale Level Set Framework for Echocardiographic Image Segmentation,” Medical Image Analysis, vol. 7, pp. 529-537, 2003.

[11] T.F. Chan, and L.A. Vese, “Active Contour and Segmentation Models Using Geometric PDE's for Medical Imaging in Malladi, R. (Ed.), “Geometric Methods in Bio-Medical Image Processing”, Series: Mathematics and Visualization, Springer, pp. 63-75, 2002.

[12] S. H. Itzkowitz, Y. S. Kim, Sleisinger & Fordtran's gastrointestinal and liver disease, 6th ed., vol. 2, Philadelphia, WB Saunders Company, 1998.

[13] E. Koike et al, “Ultrasonographic Characteristics of Thyroid Nodules: Prediction of Malignancy”, Archives of Surgery, vol. 136, pp. 334-337, 2001.

[14] S. Theodoridis, and K. Koutroumbas, “Pattern Recognition”, Academic Press, 1998.